# Vancomycin-Modified Mesoporous Silica Nanoparticles for Selective Recognition and Killing of Pathogenic Gram-Positive Bacteria Over Macrophage-Like Cells

**ARTICLE** *in* ACS APPLIED MATERIALS & INTERFACES · OCTOBER 2013

Impact Factor: 6.72 · DOI: 10.1021/am403940d · Source: PubMed



**4 AUTHORS**, INCLUDING:

Li-Li Li
National Center for Nanoscience and Technol…
**21** PUBLICATIONS **201** CITATIONS
SEE PROFILE

Hao Wang
National Center for Nanoscience and Technol…
**101** PUBLICATIONS **1,727** CITATIONS
SEE PROFILE

ACS APPLIED MATERIALS & INTERFACES

Research Article

www.acsami.org

# Vancomycin-Modified Mesoporous Silica Nanoparticles for Selective Recognition and Killing of Pathogenic Gram-Positive Bacteria Over Macrophage-Like Cells

Guobin Qi,[†,‡,§] Lili Li,[‡,§] Faquan Yu,[*,†] and Hao Wang[*,‡]

[†]Key Laboratory for Green Chemical Process of Ministry of Education, School of Chemical Engineering and Pharmacy, Wuhan Institute of Technology, No. 693 Xiongchu Avenue, Hongshan, wuhan 430073, China

[‡]Laboratory for Biological Effects of Nanomaterials and Nanosafety, National Center for Nanoscience and Technology (NCNST), No. 11 Beiyitiao, Zhongguancun, Beijing 100090, China

Supporting Information

**ABSTRACT:** Rapid, reliable recognition and detection of bacteria from an authentic specimen have been gained increasing interests in the past decades. Various materials have been designed and prepared for implementation of bacterial recognition and treatment in the artificial systems. However, in the complicated physiological condition, the macrophages always compromise the outcomes of bacterial detection and/or treatment. In this work, we demonstrated the vancomycin-modified mesoporous silica nanoparticles (**MSNs⊂Van**) for efficiently targeting and killing gram-positive bacteria over macrophage-like cells. Owing to the specific hydrogen bonding interactions of vancomycin toward the terminal D-alanyl-D-alanine moieties of gram-positive bacteria, the **MSNs⊂Van** exhibited enhanced recognition for gram-positive bacteria due to the multivalent hydrogen binding effect. Furthermore, the fluorescent molecules (FITC) were covalently decorated inside of mesopores of MSNs for tracking and visualizing the **MSNs⊂Van** during the detection/treatment processes. Upon incubation of FITC decorated MSNs with bacteria (i.e., *S. aureus* and *E. coli* as gram-positive and gram-negative bacteria, respectively) or macrophage-like cells (Raw 264.7), the fluorescence signals in *S. aureus* were 2−4 times higher than that in *E. coli* and no detectable fluorescence signals were observed in Raw 264.7 cells under the same condition. Finally, the **MSNs⊂Van** showed unambiguous antibacterial efficacy without decrease in cell viability of macrophage-like cells. This new strategy opens a new door for specific detection and treatment of pathogenic bacteria with minimized side effects.

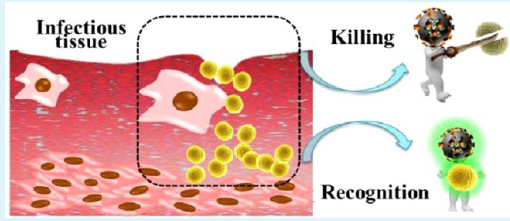


**KEYWORDS:** *mesoporous silica nanoparticle, recognition, antibacterial, macrophage-like cells, vancomycin*

## 1. INTRODUCTION

Bacterial infections are one of the most serious risks in public health in the world. Extensive efforts have been devoted to develop convenient and rapid methods for detection and identification of bacteria.[1−3] Current diagnostic techniques such as bacterial culture,[4] biochemical staining,[5] and polymerase chain reaction (PCR)[6,7] are slow, expensive, or complicated. They are not practical for reliable and specific bacteria identification in the clinical specimen.[8−10] Diagnostic of bacterial infection usually needs separation, enrichment, and identification of rare bacteria from a large quantity of fluids such as blood, urine, and saliva. The whole procedure is generally time-consuming, unreliable and low reproducible. Quantitative real-time PCR (qPCR) as a highly sensitive tool has shown particular promise for bacterial species identification.[11−13] However, qPCR-based systems are often too expensive for resource-limited environments, and current sequencing techniques still lack practical applicability to patient care.[14−16]

Macrophages, a kind of white blood cell, are the first cells at the scene of bacterial infection. The infected tissues call for help by releasing chemicals to attract macrophages, which can engulf viruses and bacteria via phagocytosis.[17] The concomitance of bacteria and macrophages upon infection becomes one of the most challenging tasks for bacterial detection and treatment. Therefore, how to selectively recognize and kill bacteria with limited damage of macrophages remains an interesting but less investigated topic so far.[18]

Mesoporous silica nanoparticles (MSNs) have been used as drug carriers or imaging probes owing to their high biocompatibility and intrinsically large drug loading capacity.[19−22] Meanwhile, MSNs can also be utilized as imaging probes by introducing optical reporters into mesoporous channels.[23−25] For example, Shi et al. reported an effective nuclear targeted drug delivery carrier using TAT peptide-conjugated monodispersed MSNs.[26] Kim et al. prepared MCM-41 typed MSNs as a nanocontainer for controlled drug delivery.[27] Besides, Zhao et al. utilize squaraine loaded MSNs

Received: July 26, 2013
Accepted: October 16, 2013
Published: October 16, 2013

  

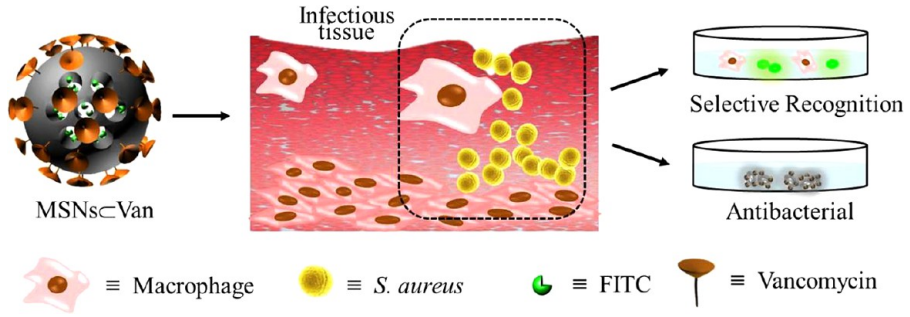


**Figure 1.** Schematic representation of **MSNs⊂Van** for selective recognition and killing pathogenic gram-positive bacteria over macrophage-like cells.

for bioimaging.[28] Inspired by those works, we attempted to employ the easily available and biocompatible MSNs for specific bacteria detection and treatment.

Various materials and technologies have been used for pathogenic bacteria detection, identification and antibacterial treatment.[20,29−31] For example, Adhya et al. described a rapid and simple method for bacterial detection in vivo, in which the biotinylated host-specific bacteriophage was labeled with streptavidin-coated quantum dots.[32] Weissleder et al. demonstrated a bioorthogonal approach for specific, selective and fast bacterial diagnosis.[33] This group also designed a magnetic gram stain method, which could be able to diagnose crude specimen without major purification. The usage of micro nuclear magnetic resonance ($\mu$NMR) device could envision rapid and sensitive detection of bacterial samples.[34] Beside sensitive and rapid detection of pathogenic bacteria, the identification is equally important. Lee and the co-workers improved their design using a novel magneto-DNA probe capable of rapid and specific profiling of pathogens directly in clinical samples.[15] Paunov et al. developed a class of selective antimicrobial agent based on the recognition of shape and size of bacterial cells to realize target and killing of bacteria concurrently.[35,36]

To enhance the detection specificity of nanoparticles toward bacteria, we usually modified the surface of nanoparticles with antibodies for targeting the bacteria.[32,37] However, the expensive and denature properties of antibodies hampered their widely application in bacterial detection.[38] Small molecules in this case might be a more attractive alternative to solve this problem. The symbolic molecules are a class of narrow-spectrum antibiotics which show strong binding affinity to bacteria.[39,40] Vancomycin is recognized as a symbolic antibiotic. The skeleton of vancomycin binds with the terminal D-alanyl-D-alanine moieties of gram-positive bacteria through hydrogen bonding interactions and the dissociation constant ($K_d$) between them is about 1−4 $\mu$M at pH 7.0.[41]

Herein, we reported dye-doped mesoporous silica nanoparticles modified by vancomycin (**MSNs⊂Van**) for selective recognition and killing of pathogenic gram-positive bacteria over macrophage-like cells (Figure 1). The fluorescent FITC molecules were covalently decorated into mesopores of MSNs for tracking the **MSNs⊂Van**. The hydrodynamic diameters of **MSNs⊂Van** are 90 ± 37 nm with a positive charged surface of +12.7 mV. The vancomycin loading capacity is 1 mg vancomycin per mg MSNs. In our previous work, we reported the lysozyme-coated mesoporous silica nanoparticles (MSNs⊂Lys) as antibacterial agents that exhibited efficient antibacterial activity.[25] In order to decrease the side effect during the treatment, in this work, the surface of MSNs was modified with vancomycin and the resulting material was endowed with targeting capability for gram-positive bacteria. The advantages of this system are (i) vancomycin corona on **MSNs⊂Van** provides multivalent interactions and enhanced specific recognition toward gram-positive bacteria over macrophage-like cells and (ii) the high local concentration of vancomycin on **MSNs⊂Van** surface enables the nanoparticles strongly immobilized in the cell walls of *S. aureus* and results in significant inhibition effect on cell wall synthesis. **MSNs⊂Van** were demonstrated to be a reliable and specific gram-positive bacteria detection probe, meanwhile they still retained the capability of antibacterial properties.

## 2. MATERIALS AND METHODS

**2.1. Materials.** Fluorescein isothiocyannate (FITC), 3-aminopropyltriethoxysilane (APS), cetyltrimethylammonium bromide (CTAB), tetraethylorthosilicate (TEOS), Vancomycin (Van), N-(3-Dimethylaminopropyl)-N′-ethylcarbodiimide hydrochloride (EDAC), N-Hydroxysuccinimide (NHS), 4-morpholineethanesulfonic acid hemisodium salt (MES), trifluoroacetic acid (TFA) were purchased from Sigma-Aldrich Chemical Co. Dulbecco's Modified Eagle Medium (DMEM), penicillin, streptomycin, fetal bovine serum (FBS) and trypsin were obtained from HyClone/Thermo fisher (Beijing, China). Raw 264.7 cell lines were purchased from Cell Culture Center of Institute of Basic Medical Sciences, Chinese Academy of Medical Sciences (Beijing, China). Inertsil C18 HPLC column (ODS-3, 3 $\mu$m, 4.6 × 150 mm) for peptide and vancomycin was purchased from GL Sciences Inc. The HPLC grade solvents were purchased from Aldrich, Fisher Scientific. Luria−Bertani broth (LB) and Tryptic Soy Broth (TSB) were obtained from Beyotime institute of biotechnology (Shanghai, China) 96-well coning culture plates were purchased from Coning Company. The bacteria strain of *Escherichia coli* (ATCC8739) and *Staphylococcus aureus* (ATCC6538) was obtained from China General Microbiological Culture Collection Center. All the other solvents used in the research were purchased from Sinopharm Chemical Reagent Beijing Co., Ltd.

**2.2. Synthesis of Mesoporous Silica Nanoparticles (MSNs).** Dye-doped MSNs were synthesized according to previous method[23] with minor modification. FITC (4 mg) was reacted with APS (44 $\mu$L) under a molar ratio of FITC:APS = 1:10 in ethanol (1 mL) overnight at room temperature in the dark. CTAB (0.1 g) was added into a NaOH aqueous solution (50 mL, 0.014 M) and the resulting mixture was heated to 70 °C under stirring. Then TEOS (0.5 mL) and the APS-conjugated FITC solution (50 $\mu$L) were added to above-prepared mixture. After the reaction was kept for 1 min under vigorous stirring, ethyl acetate (0.5 mL) was added and the resulting mixture was reacted for another 30 s and followed up with 2 h aging. The precipitate was collected by centrifugation, washed with water, and ethanol at least three times and dried under vacuum overnight.

**2.3. Surface Modification of MSNs.** The surface of MSNs was functionalized with amino groups. MSNs (0.1 g) were dispersed in ethanol (10 mL), followed by the addition of APS (40 $\mu$L) and the resultant mixtures were refluxed for 3 h. The precipitate was centrifuged and washed with ethanol three times. Afterward, the

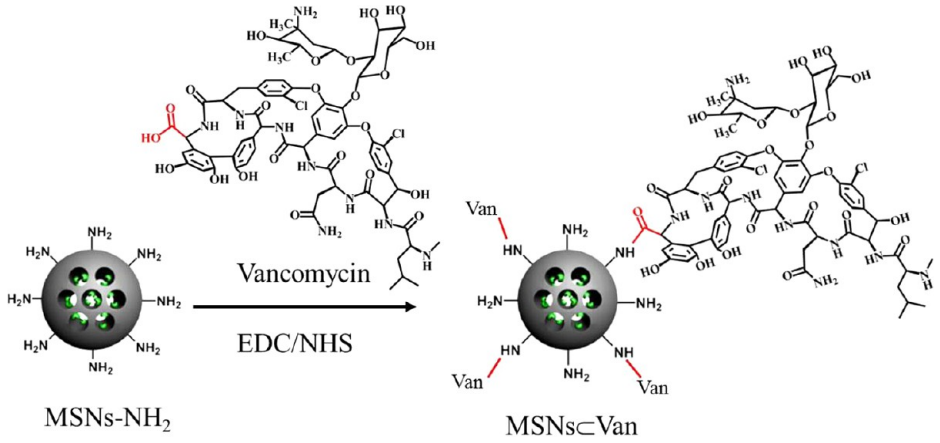


**Figure 2.** Synthetic procedure of **MSNs⊂Van**.

pore-generating template CTAB was removed by refluxing the MSNs in HCl and ethanol (50 mL, 1:9, v: v) under 60 °C, The product was collected by centrifugation and washed with a mixture of ethanol, water, and sodium bicarbonate (20 mL: 20 mL: 250 $\mu$g).

**2.3. Synthesis of Vancomycin-Modified MSNs (MSNs⊂Van).** The vancomycin was mixed with NHS and EDC in a MES buffer solution (50 mM, pH 5.5) in a molar ratio of 1:4:4. The NHS-vancomycin was obtained by purified by preparative reverse-phase HPLC (0.025 M potassium dihydrogen phosphate buffer/methanol 80/20 v/v over 20 min, $R_f$ = 9.2 min). Then, the purified NHS-vancomycin (30 mg) and amine-functionalized MSNs (20 mg) were mixed in 30 mL of Millipore water under an ice bath and stirred for 3 h. The free NHS-vancomycin was removed by centrifugation. The precipitate was then gently washed by water triplicate until there was no free NHS-vancomycin detected in the supernatant.

**2.4. Characterizations of MSNs⊂Van.** The morphology and sizes of MSNs and **MSNs⊂Van** were directly examined using a transmission electron microscope. The studies were carried out on a Tecnai G2 F20 U-TWIN high-resolution electron microscope operating at an accelerating voltage of 200 keV. The TEM samples were prepared by performing drop-coating of MSNs or **MSNs⊂Van** solutions (2 $\mu$ L) onto carbon-coated copper grids. After contacting the droplets with copper grids for 45 s, excess droplets were removed using filter papers. All samples were dried under vacuum before the TEM studies. The photoluminescence spectra were recorded in a quartz cuvette (10 × 10 mm), using a Tianjin Gangdong F-280 spectrophotometer with excitation wavelength set at 488 nm. Absorption spectra were recorded in a quartz cuvette (10 × 10 mm), using a Shimadzu UV-2600 UV−vis spectrophotometer and were corrected for the solvent absorption. DLS experiments were performed with Zetasizer Nano ZS instrument. MSNs and **MSNs⊂Van** samples for DLS were diluted with PBS buffer solution (pH 6.2) to 1 mg $mL^{-1}$ to make intensities in the range suitable for scattering. The sizes and standard derivations of MSNs and **MSNs⊂Van** were calculated by average values of at least triple measurements. Zeta potentials ($\zeta$) of MSNs and **MSNs⊂Van** were determined by photon correlation spectroscopy using a Zetasizer Nano instrument (Malvern Instruments, Malvern, UK). The measurements were performed at 25 °C with a detection angle of 90° and the raw data were subsequently correlated to Z average mean size using a cumulative analysis by the Zetasizer software package.

**2.5. Scanning Electron Microscope (SEM).** The morphologies of **MSNs⊂Van** interacting with *E. coli* and *S. aureus* were directly examined using scanning electron microscope. The studies were carried out on a Tecnai G2 F20 U-TWIN high-resolution electron microscope operating at an accelerating voltage of 200 keV. The SEM samples were prepared by performing drop-coating of bacteria or **MSNs⊂Van** interacting bacteria solutions (2 $\mu$L) onto silicon wafer. After contacting the droplets with silicon wafer for 45 s, an excess amount of droplets were removed by filter papers. Subsequently, the bacteria were solidified with glutaraldehyde (4%) overnight and then coated by gold before scanning.

**2.6. Determination of Vancomycin Loading.** Vancomycin loading amount was measured by subtracting the unreacted vancomycin in the supernatant from the added total amount. The unreacted vancomycin in the supernatant was quantified by a high-performance liquid chromatography (HPLC, Waters 2796) with a dual $\lambda$ absorbance detector and a C18 column (Inertsil ODS-3, 3 $\mu$m, 4.6 × 150 mm). The calibration curve of vancomycin was determined by plotting the integration of peak area with retention time at 6.5 min vs the concentrations of vancomycin. The peak area of vancomycin was detected at 230 nm with a mobile phase of 0.025 M potassium dihydrogen phosphate buffer and methanol (80:20, v: v).

**2.7. Minimum Inhibitory Concentration (MIC).** *E. coli* and *S. aureus* were respectively cultured in the LB medium and TSB medium at 37 °C on a shaker bed at 200 rpm for 4−6 h. Then the concentration of bacteria, corresponding to an optical density of 0.1 at 600 nm for 1 × $10^8$ CFU $mL^{-1}$ diluted with the medium, was measured by UV−vis spectroscopy (Cary100Bio). We added bacterial suspension (20 $\mu$L of 1 × $10^6$ CFU $mL^{-1}$) medium (140 $\mu$L) for each well. Then PBS (20 $\mu$L, as the blank control), Van, MSNs, and **MSNs⊂Van** were separately added into 96-well plates and shaken at 37 °C on a shaker bed with 200 rpm for 18 h. The bacterial viability was determined by OD600 nm using multifunctional microplate reader (Tecan infinite M200). Each concentration was prepared and measured in triplicate, and all experiments were repeated at least twice in parallel.

**2.8. Confocal Laser Scanning Microscopy (CLSM).** The same concentration of **MSNs⊂Van** (50 $\mu$g $mL^{-1}$) were incubated with respective Raw 264.7 cells (1 × $10^5$ cells $cm^{-2}$), *E. coli* (1 × $10^8$ CFU $mL^{-1}$) and/or *S. aureus* (1 × $10^8$ CFU $mL^{-1}$) in PBS in glass bottom dishes at 37 °C for 30 min. The bacteria in supernatant were harvested by centrifugation (3000 rpm for 5 min) and the pellets were suspended in PBS and the suspensions were kept at 4 °C for CLSM characterization. The adhesive Raw 264.7 cells were washed by PBS triplicated. Individual aliquots of 10 $\mu$L of the preprepared mixed suspensions were added to clean glass bottom dishes followed by slightly covering coverslips for immobilization. The specimens were examined by confocal laser scanning microscopy with a × 100 oil-immersion objective lens using a 488 nm laser (Carl Zeiss AG, LSM780).

**2.9. Mouse Infection Model.** Animals were maintained in the Center for Experimental Animals (an AAALAC-accredited experimental animal facility) at Peking University. All procedures involving experimental animals were performed in accordance with protocols approved by the Committee for Animal Research of Peking University, China. To evaluate the in vivo antibacterial effect of **MSNs⊂Van**, the *S. aureus* infection model was built. Nine female BALB/c mice (6−8 weeks, 18−22 g) were purchased from Vital River Laboratory Animal Technology Co. Ltd. and allowed to acclimatize for three days in the

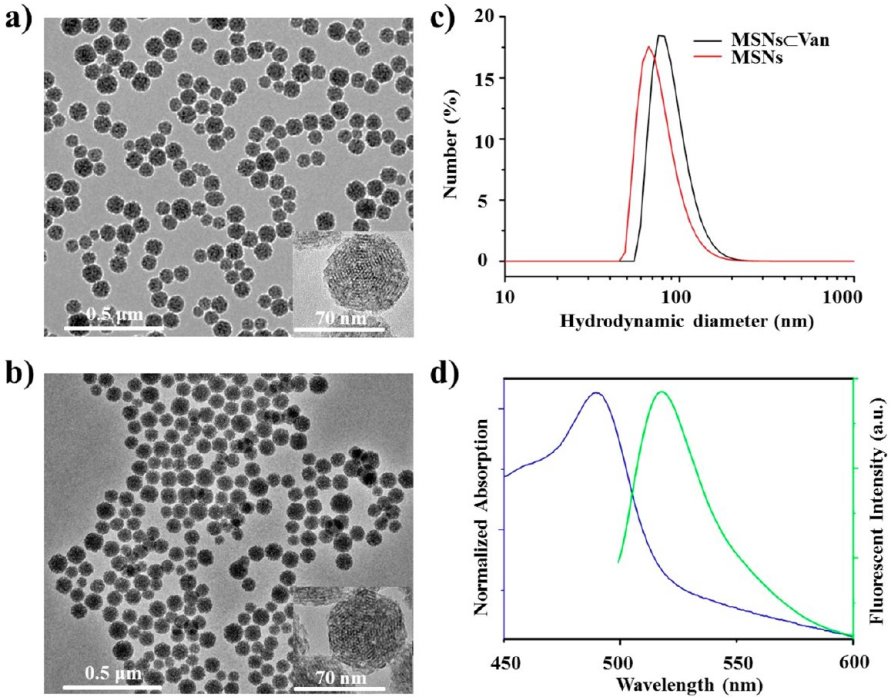


**Figure 3.** Characterizations of **MSNs⊂Van.** TEM images of (a) MSNs and (b) **MSNs⊂Van**. (c) Hydrodynamic diameters and distribution of MSNs and **MSNs⊂Van** measured by DLS in PBS buffer (pH 6.8). (d) Fluorescence emission spectrum (green line) and UV spectrum (blue line) of **MSNs⊂Van** with a concentration of 1 mg $mL^{-1}$. Excitation wavelength is 488 nm.

lab. Approximately $2 \times 10^6$ CFU of *S. aureus* washed with sterile PBS and resuspended in sterile PBS (50 $\mu$L) were injected by subcutaneous injection and infected in vivo for 24 h before treatment. The three groups of mice (three mice per group) were divided into PBS, MSNs, and **MSNs⊂Van** groups. The **MSNs⊂Van** and control groups were injected once a day and a dose of 50 $\mu$L (500 $\mu$g $mL^{-1}$). After five days, all mice were sacrificed and the infected tissues were processed for further analysis. To determine the amount of *S. aureus* in the infected tissues of the mice, the tissues were homogenized in sterile PBS (5 mL) containing 1% Triton X-100. Aliquots of diluted homogenized infected tissues were plated on agar, on which the grown colonies were counted for analysis.

## 3. RESULTS AND DISCUSSION

**3.1. Synthesis of Vancomycin-Modified Dye-Doped MSNs.** The MSNs were prepared according to a reported method.[23] Briefly, fluorescein isothiocyanate (FITC) was first in situ doped into the cavities of the MSNs through the formation of a thioureido bond. Then amino modification on the surface of MSNs was coupled by 3-aminopropyltriethoxysilane (APS). Simultaneously, the carboxyl group of vancomycin was activated by N-(3-Dimethylaminopropyl)-N′-ethylcarbodiimide hydrochloride (EDAC) and N-Hydroxysuccinimide (NHS) in 4-morpholineethanesulfonic acid hemisodium salt (MES) buffer (50 mM, pH 5.5). After that, the NHS-vancomycin was obtained by purified the upper solution via preparative reverse-phase HPLC (2535, Waters, with C18 column and UV detector). These amine-modified nanoparticles can be quantitatively reacted with NHS-vancomycin. Finally, the vancomycin-modified dye-doped MSNs (**MSNs⊂Van**) (Figure 2) were purified by centrifugation at 10000 rpm. The amount of vancomycin was quantified by the reverse-phase HPLC with the retention time of 6.5 min in PBS. The estimated quantity of immobilized vancomycin on the surface of MSNs was determined by subtraction of vancomycin in the supernatant from the total feeding amount (see the Supporting Information, Figure S1). The experimental results show that the vancomycin loading capacity is 1 mg vancomycin per mg MSNs (1 mg Van/1 mg MSNs).

**3.2. Characterizations of MSNs⊂Van.** The morphology and size of the MSNs and **MSNs⊂Van** were examined by transmission electron microscopy (TEM, Tecnai G2 20 S-TWIN).[42−44] The TEM images suggest that the MSNs are uniform sphere with a narrow size distribution (Figure 3a). The size of the resulting MSNs was 65 ± 10 nm based on the TEM images (calculated more than 200 particles). After modification of vancomycin on the surface, there is almost no obvious change on the morphology and size of the **MSNs⊂Van** (Figure 3b). Furthermore, the hydrodynamic diameter of MSNs and **MSNs⊂Van** were measured by dynamic light scattering (DLS, Zetasizer Nano ZS, Malvern). The results indicate that the hydrodynamic diameters of MSNs and **MSNs⊂Van** are 77 ± 23 and 90 ± 37 nm, respectively (Figure 3c). Note that vancomycin covalently bonding modification on the surface lead to minor variations on the hydrodynamic diameter. Besides, the functional molecules on MSNs did not affect the polydispersity index (PDI) of the nanoparticles which still retain lower than 0.15. Accordingly, the zeta potential ($\zeta$) of **MSNs⊂Van** dropped to +12.7 mV upon coating of the vancomycin corona (+38.5 mV for MSNs, see the Supporting Information, Figure S2). Because of the doping of FITC into the mesopores of **MSNs⊂Van**, these nanoparticles showed a maximum absorption wavelength at 488 nm (measured by UV spectrometer, UV-2600, Shimadzu) and strong FITC emission at 520 nm (measured by fluorescence spectrometer, F-280, Tianjin Gangdong Co., Ltd.), which enable to tracking the nanoparticles in bacteria (Figure 3d).

**3.3. Selective Recognition of Gram-Positive Bacteria to Gram-Negative Bacteria.** In order to directly visualize the selective recognition of gram-positive bacteria in a mixture of

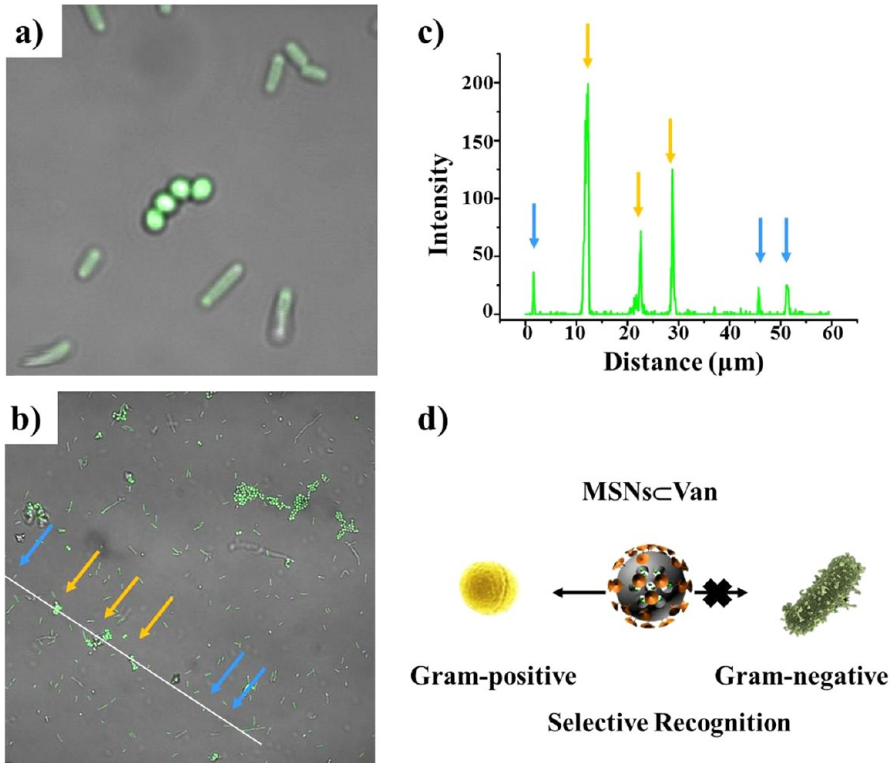


**Figure 4.** CLSM measurements of the mixture of *S. aureus* and *E. coli* treated by **MSNs⊂Van**. (a) Overlay images of mixture of *S. aureus* and *E. coli* treated by **MSNs⊂Van**; (b) large-scale CLSM images. The orange arrows and blue arrows indicated *S. aureus* cells and *E. coli* cells, respectively; (c) fluorescence intensity profiling of *S. aureus* and *E. coli* ; (d) schematic representation of selectivity of **MSNs⊂Van** for two bacterial species.

gram-positive (*S. aureus*) and gram-negative (*E. coli*) bacteria, confocal laser scanning microscopy (CLSM) was utilized. In the high-magnification CLSM images (×40 000, Figure 4a), the *S. aureus* shows higher fluorescence intensity than that in *E. coli* The vancomycin modified on the **MSNs⊂Van** could form a five-point hydrogen bond interaction with the terminal D-Ala-D-Ala moieties of the $\beta$-1,4-linked N-acetylglucsamine (NAG) and N-acetylmuramic acid (NAM) peptide on the *S. aureus* membrane.[41] The weak fluorescence signal in *E. coli* is attributed to the nonspecific electrostatic interaction between **MSNs⊂Van** and *E. coli*. To realize the rapid identification of gram-positive bacteria form gram-negative bacteria, the low-magnification confocal image and its line scanning profiles of the mixture of *S. aureus* and *E. coli* were carried out (×6000, Figure 4b, c). The line scanning profiles of fluorescence intensity in the selected bacterial cells further confirm the specific recognition of *S. aureus* over *E. coli* (Figure 4d). The intensity of the fluorescence in *S. aureus* (orange arrows) was 2−4 times than that in *E. coli* (blue arrows) (Figure 4b, c). The specific recognition of **MSNs⊂Van** for *S. aureus* over *E. coli* was confirmed by scanning electron microscope (SEM) studies. After treatments of bacteria samples by **MSNs⊂Van** with a concentration of 200 $\mu$g mL$^{-1}$ for 2 h, the **MSNs⊂Van**, *S. aureus* and *E. coli* ($1 \times 10^5$ CFU mL$^{-1}$) can be readily distinguished by morphology and size. *S. aureus* and *E. coli* showed spherical and cylindrical morphologies in microscale (Figure 5a, b). Compared to untreated group, *S. aureus* cells were heavily surrounded by **MSNs⊂Van** because the strong specific hydrogen bonding interactions between the well-orientated vancomycin moieties on the surface of **MSNs⊂Van** and *S. aureus* cell walls (Figure 5c). Meanwhile, the lower adhesion of **MSNs⊂Van** on gram-negative bacteria of *E. coli*

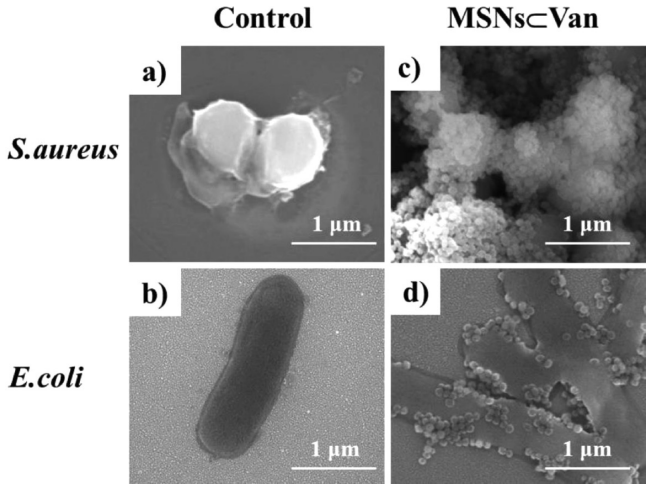


**Figure 5.** SEM images of *S. aureus* and *E .coli*. (a, b) *S. aureus* and *E .coli* ($1 \times 10^5$ CFU mL$^{-1}$) suspended in PBS as control groups; (c, d) Images of *S. aureus* and *E .coli* treated by **MSNs⊂Van** with a concentration of 200 $\mu$g mL$^{-1}$ for 2 h, respectively.

(Figure 5d) was attributed to the electrostatic interaction of the positively charged **MSNs⊂Van** and negatively charged bacterial membrane surface.

**3.4. Selective Recognition of Gram-Positive Bacteria over Macrophage-like Cells.** In term of cell selection, the mouse leukemic monocyte macrophage cell line (Raw 264.7) was chosen for mimic the macrophage cells infectious tissue environment. The Raw 264.7 cells were incubated with *S. aureus* and *E. coli* separately, and then the **MSNs⊂Van** were added and the resulting mixtures were incubated for another 30

min in PBS. The targetability of **MSNs⊂Van** toward different species was studied by CLSM. As can be seen from Figures 6a and b, upon treatment of a mixture of *S. aureus* and Raw 264.7 macrophages with **MSNs⊂Van**, the *S. aureus* showed significant fluorescence intensity compared to that of the Raw 264.7 cells. In parallel, under the same culture condition and images acquiring parameters, the fluorescence signals of **MSNs⊂Van** on the *E. coli* are capable of observed slightly (Figure 6c, d). The significant recognition effect of **MSNs⊂Van** toward *S. aureus* is attributed to the targeting capability of vancomycin through multivalent hydrogen bonding interactions. In sharp contrast, no detectable binding between **MSNs⊂Van** and Raw 264.7 cells was found. This is due to the asymmetric interaction of negatively charged phosphatidylserine (PS) of Raw 264.7 cells, which is mainly located in the inner leaflet of plasma membrane, makes membrane of Raw 264.7 macrophage cells closer to electrically neutral.[45] We deduced that the driving force of the weak association between **MSNs⊂Van** and *E. coli* was electrostatic interaction. Because, the main composition of bacterial cell walls of peptidoglycan exhibits net negative charged on the membrane surface.[45] The surface positive changed of **MSNs⊂Van** with a zeta potential of +12.7 mV make the nanoparticles more easily electrostatic adsorbed onto the bacterial cell wall than macrophage-like cells.

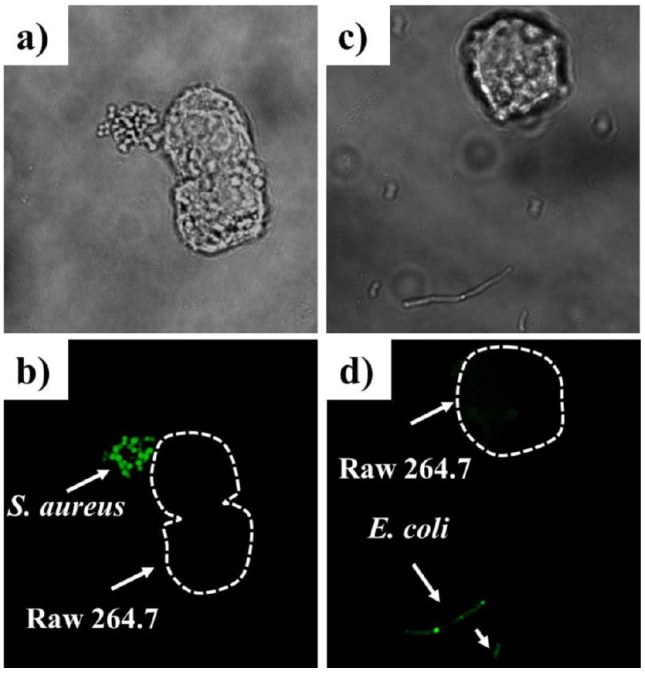


**Figure 6.** CLSM images of (a, b) the mixtures of Raw 264.7 cells and *S. aureus* incubated with **MSNs⊂Van** for 30 min; (c, d) the mixtures of Raw 264.7 cells and *E. coli* incubated with **MSNs⊂Van** for 30 min. Top, bright-field images; bottom, fluorescence images.

**3.5. Antibacterial Capability and Biocompatibility of MSNs⊂Van.** Vancomycin is a kind of antibiotic, which is effective for inhibition the growth of gram-positive bacteria. It is well-known that the vancomycin interacts with gram-positive cells through a surprisingly simple five-hydrogen bond motif between the heptapeptide backbone of vancomycin and D-Ala-D-Ala dipeptide extending from the cell wall.[41] The antibacterial capability of **MSNs⊂Van** was tested by culture of *S. aureus* and **MSNs⊂Van** with different concentrations for 18 h. We are satisfied that **MSNs⊂Van** showed entirely inhibition of *S. aureus* growth with a minimum inhibitory concentration (MIC) of 200 $\mu$g mL$^{-1}$ (see the Supporting Information, Figure S3). Meanwhile, there is no antibacterial activity observed upon the concentration of MSNs up to 500 $\mu$g mL$^{-1}$ (see the Supporting Information, Figure S4). The selective antibacterial capability over macrophage-like cells was confirmed by fluorescence microscope images (fluorescence microscope, Cri Nuance TM). The Raw 264.7 cells and S. *aureus* were incubated with **MSNs⊂Van** (with a concentration of 200 $\mu$g mL$^{-1}$) for 12 h and then the dead cells were stained with PI (Figure 7a).

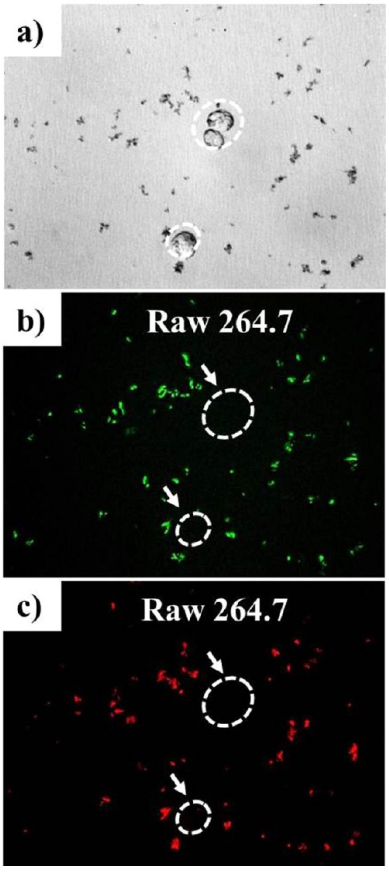


**Figure 7.** Mmicroscope images of Raw 264.7 cells and *S. aureus* incubated with **MSNs⊂Van** for 12 h and then stained with PI. (a) Bright-field image of the mixture of Raw 264.7 and *S. aureus*; (b) green fluorescence signals (488 nm excitation) from the **MSNs⊂Van**; and (c) red fluorescence signals (568 nm excitation) from the PI-stained dead bacteria.

Corresponding to the selective recognition of gram-positive bacteria over macrophage-like cells, **MSNs⊂Van** were hydrogen bonding onto *S. aureus* and lighted up the bacterial cells with green fluorescence (Figure 7b). The dead cells (red spots) were well overlay with **MSNs⊂Van** signals (Figure 7c). The Raw 264.7 (inside white circles) have no fluorescence signal, implying no binding effect on macrophage-like cells by **MSNs⊂Van**. The good biocompatibility of **MSNs⊂Van** also confirmed by cell viability assay by using human embryonic kidney (293T) and human hepatocytes (LO2) (see the Supporting Information, Figure S5). The antibacterial mechanism of vancomycin is due to its inhibition capability for bacterial cell wall synthesis,[39,46] and therefore vancomycin-based materials always show time-dependent antibacterial efficacy. In order to clarify this issue, the time-dependent

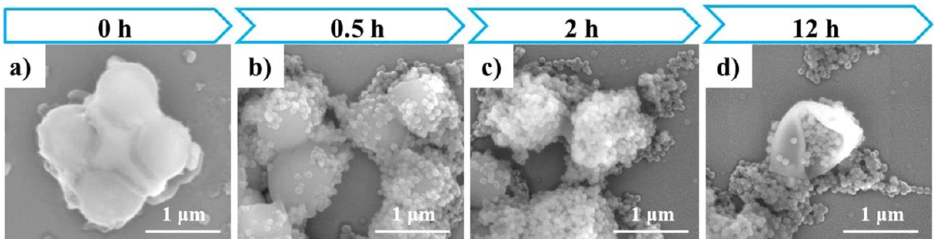


**Figure 8.** Time-dependent morphological changes of *S. aureus* cells treated with **MSNs⊂Van**. The typical SEM images of *S. aureus* ($1 \times 10^5$ CFU $mL^{-1}$) treated with **MSNs⊂Van** (200 $\mu$g $mL^{-1}$) are presented at different time points at 0, 0.5, 2, and 12 h.

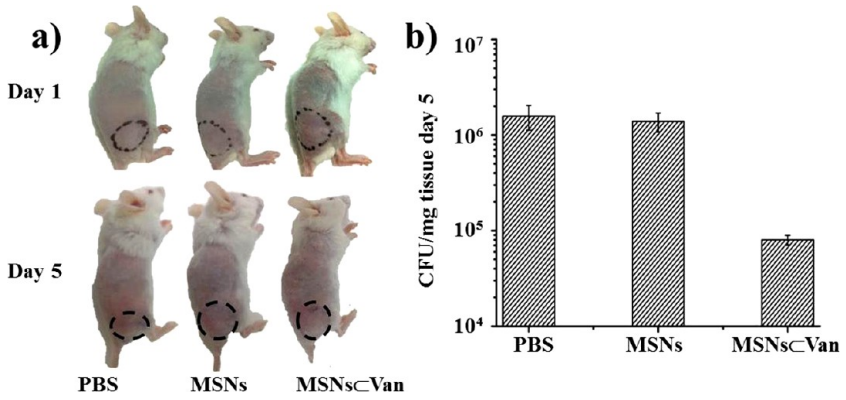


**Figure 9.** Evaluation of antibacterial activity in vivo. (a) Photos of *S. aureus* infected mice at day 1 and day 5 after infection. Three groups of mice (three mice per group) were divided into PBS, MSNs, and **MSNs⊂Van** groups. The groups treated with PBS, MSNs, and **MSNs⊂Van** (50 $\mu$L, 500 $\mu$g $mL^{-1}$) once a day for 4 days. (b) Surviving *S. aureus* in the infected tissues were quantified on the 5th day. Error bars are taken from three mice per group.

SEM studies were carried out to monitor the interactions between **MSNs⊂Van** and *S. aureus* (Figure 8a–d). The **MSNs⊂Van** rapidly recognize and subsequently adhere onto the surface of *S. aureus* at the first 30 min. More **MSNs⊂Van** were coated on the *S. aureus* to form thick **MSNs⊂Van** layers after 2 h. The cell walls/membranes of *S. aureus* started to collapse, indicating that the bacterial cell wall synthesis was inhibited after 12 h which ultimately led to the death of bacteria. The in vivo experiments of **MSNs⊂Van** were carried out to evaluate the antibacterial activity of **MSNs⊂Van**. The three groups of mice (three mice per group) were divided into PBS, MSNs, and **MSNs⊂Van** groups. Compared to the control groups (PBS and MSNs), the **MSNs⊂Van** showed remarkable antibacterial activity and 10 times decrease of bacteria in the infected tissues were observed 5 days post administration of **MSNs⊂Van** compared to the control groups treated with PBS or MSNs (Figure 9a, b).

## 4. CONCLUSION

In summary, we designed dye-doped **MSNs⊂Van** which were modified by vancomycin for selective recognition and killing pathogenic gram-positive bacteria over macrophage-like cells. The specific hydrogen bonding interactions between vancomycin of **MSNs⊂Van** and terminal D-Ala-D-Ala moieties of gram-positive bacteria cell wall lead to the selective recognition of gram-positive bacteria. No detectable nonspecific binding of **MSNs⊂Van** with macrophage-like cells was observed. Meanwhile, the weak recognition of **MSNs⊂Van** with gram-negative bacteria was found, which is attributed to the nonspecific electrostatic interactions between **MSNs⊂Van** and negatively charged bacterial membranes. Finally, the **MSNs⊂Van** can not only specifically detect gram-positive bacteria but also effectively inhibit the growth of bacteria without interference of cellular activity of macrophage cells. This strategy might realize the detection of bacterial infection with high sensitivity, specificity, and enhanced antibacterial capability with minimized side effect.

## ■ ASSOCIATED CONTENT

### Supporting Information

Experimental details including the calibration curve of vancomycin concentrations, zeta potential, antibacterial activity of MSNs and **MSNs⊂Van**, and cell viability assay. This material is available free of charge via the Internet at http://pubs.acs.org.

## ■ AUTHOR INFORMATION

### Corresponding Authors

*E-mail: fyu@mail.wit.edu.cn. Tel: 86-27-87194980.
*E-mail: wanghao@nanoctr.cn. Tel: 86-10-82545759.

### Author Contributions

§G.Q. and L.L. contributed equally to this work. All authors have given approval to the final version of the manuscript.

### Notes

The authors declare no competing financial interest.

## ■ ACKNOWLEDGMENTS

This work was supported by National Basic Research Program of China (973 Program, 2013CB932701), the 100-Talent Program of the Chinese Academy of Sciences, Beijing Natural Science Foundation (2132053), and the National Natural Science Foundation of China (Grant 21071114).

## ■ REFERENCES

(1) Xie, X.; Xu, W.; Liu, X. *Acc. Chem. Res.* **2012**, *45*, 1511–1520.

(2) Lin, M.; Pei, H.; Yang, F.; Fan, C.; Zuo, X. *Adv. Mater.* **2013**, *25*, 3490−3496.
(3) Yang, L.; Yan, B.; Premasiri, W. R.; Ziegler, L. D.; Negro, L. D.; Reinhard, B. M. *Adv. Funct. Mater.* **2010**, *20*, 2619−2628.
(4) Huddleson, I. F.; Baltzer, B. *Science* **1950**, *112*, 651−652.
(5) Gao, J.; Li, L.; Ho, P. L.; Mak, G. C.; Gu, H.; Xu, B. *Adv. Mater.* **2006**, *18*, 3145−3148.
(6) Reller, L. B.; Weinstein, M. P.; Petti, C. A. *Clin. Infect. Dis.* **2007**, *44*, 1108−1114.
(7) Mothershed, E. A.; Whitney, A. M. *Clin. Chim. Acta* **2006**, *363*, 206−220.
(8) Giljohann, D. A.; Mirkin, C. A. *Nature* **2009**, *462*, 461−464.
(9) Sauer, S.; Kliem, M. *Nat. Rev. Microbiol.* **2010**, *8*, 74−82.
(10) Li, Y.; Cu, Y. T. H.; Luo, D. *Nat. Biotechnol.* **2005**, *23*, 885−889.
(11) Pechorsky, A.; Nitzan, Y.; Lazarovitch, T. *J. Microbiol. Methods* **2009**, *78*, 325−330.
(12) Ottesen, E. A.; Hong, J. W.; Quake, S. R.; Leadbetter, J. R. *Science* **2006**, *314*, 1464−1467.
(13) Loman, N. J.; Constantinidou, C.; Chan, J. Z. M.; Halachev, M.; Sergeant, M.; Penn, C. W.; Robinson, E. R.; Pallen, M. J. *Nat. Rev. Microbiol.* **2012**, *10*, 599−606.
(14) Loman, N. J.; Misra, R. V.; Dallman, T. J.; Constantinidou, C.; Gharbia, S. E.; Wain, J.; Pallen, M. J. *Nat. Biotechnol.* **2012**, *30*, 434−439.
(15) Chung, H. J.; Castro, C. M.; Im, H.; Lee, H.; Weissleder, R. *Nat. Nanotechnol.* **2013**, *8*, 369−375.
(16) Niemz, A.; Ferguson, T. M.; Boyle, D. S. *Trends Biotechnol.* **2011**, *29*, 240−250.
(17) Murray, P. J.; Wynn, T. A. *Nat. Rev. Immunol.* **2011**, *11*, 723−737.
(18) Liu, L.; Yang, J.; Xie, J.; Luo, Z.; Jiang, J.; Yang, Y. Y.; Liu, S. *Nanoscale* **2013**, *5*, 3834−3840.
(19) Wang, L.; Li, L.-L.; Ma, H. L.; Wang, H. *Chin. Chem. Lett.* **2013**, *24*, 351−358.
(20) Lee, J. E.; Lee, N.; Kim, T.; Kim, J.; Hyeon, T. *Acc. Chem. Res.* **2011**, *44*, 893−902.
(21) Trewyn, B. G.; Slowing, I. I.; Giri, S.; Chen, H.-T.; Lin, V. S. Y. *Acc. Chem. Res.* **2007**, *40*, 846−853.
(22) Wang, L.; Li, L.-l.; Fan, Y.-s.; Wang, H. *Adv. Mater.* **2013**, *25*, 3888−3898.
(23) Lee, J. E.; Lee, N.; Kim, H.; Kim, J.; Choi, S. H.; Kim, J. H.; Kim, T.; Song, I. C.; Park, S. P.; Moon, W. K.; Hyeon, T. *J. Am. Chem. Soc.* **2009**, *132*, 552−557.
(24) Slowing, I. I.; Trewyn, B. G.; Giri, S.; Lin, V. S. Y. *Adv. Funct. Mater.* **2007**, *17*, 1225−1236.
(25) Li, L.-l.; Wang, H. *Adv. Healthcare. Mater.* **2013**, *2*, 1351−1360.
(26) Pan, L.; He, Q.; Liu, J.; Chen, Y.; Ma, M.; Zhang, L.; Shi, J. *J. Am. Chem. Soc.* **2012**, *134*, 5722−5725.
(27) Kim, H.; Kim, S.; Park, C.; Lee, H.; Park, H. J.; Kim, C. *Adv. Mater.* **2010**, *22*, 4280−4283.
(28) Sreejith, S.; Ma, X.; Zhao, Y. *J. Am. Chem. Soc.* **2012**, *134*, 17346−17349.
(29) Coll, C.; Bernardos, A.; Martínez-Máñez, R.; Sancenón, F. *Acc. Chem. Res.* **2012**, *46*, 339−349.
(30) Tarn, D.; Ashley, C. E.; Xue, M.; Carnes, E. C.; Zink, J. I.; Brinker, C. J. *Acc. Chem. Res.* **2013**, *46*, 792−801.
(31) Massad-Ivanir, N.; Shtenberg, G.; Zeidman, T.; Segal, E. *Adv. Funct. Mater.* **2010**, *20*, 2269−2277.
(32) Edgar, R.; McKinstry, M.; Hwang, J.; Oppenheim, A. B.; Fekete, R. A.; Giulian, G.; Merril, C.; Nagashima, K.; Adhya, S. *Proc. Natl. Acad. Sci. U.S.A.* **2006**, *103*, 4841−4845.
(33) Chung, H. J.; Reiner, T.; Budin, G.; Min, C.; Liong, M.; Issadore, D.; Lee, H.; Weissleder, R. *ACS Nano* **2011**, *5*, 8834−8841.
(34) Budin, G.; Chung, H. J.; Lee, H.; Weissleder, R. *Angew. Chem., Int. Ed.* **2012**, *51*, 7752−7755.
(35) Borovička, J.; Metheringham, W. J.; Madden, L. A.; Walton, C. D.; Stoyanov, S. D.; Paunov, V. N. *J. Am. Chem. Soc.* **2013**, *135*, 5282−5285.
(36) Zhang, D.; Zhao, Y.-X.; Gao, Y.-J.; Gao, F.-P.; Fan, Y.-S.; Li, X.-J.; Duan, Z.-Y.; Wang, H. *J. Mater. Chem. B* **2013**, *1*, 5100−5107.
(37) Tseng, Y.-T.; Chang, H.-Y.; Huang, C.-C. *Chem. Commun.* **2012**, *48*, 8712−8714.
(38) Fernandes, R.; Roy, V.; Wu, H.-C.; Bentley, W. E. *Nat. Nanotechnol.* **2010**, *5*, 213−217.
(39) Jose, B.; Antoci, V., Jr.; Zeiger, A. R.; Wickstrom, E.; Hickok, N. J. *Chem. Biol.* **2005**, *12*, 1041−1048.
(40) Antoci, V.; King, S. B.; Jose, B.; Parvizi, J.; Zeiger, A. R.; Wickstrom, E.; Freeman, T. A.; Composto, R. J.; Ducheyne, P.; Shapiro, I. M.; Hickok, N. J.; Adams, C. S. *J. Orthop. Res.* **2007**, *25*, 858−866.
(41) Kell, A. J.; Stewart, G.; Ryan, S.; Peytavi, R.; Boissinot, M.; Huletsky, A.; Bergeron, M. G.; Simard, B. *ACS Nano* **2008**, *2*, 1777−1788.
(42) Ahire, J. H.; Wang, Q.; Coxon, P. R.; Malhotra, G.; Brydson, R.; Chen, R.; Chao, Y. *ACS Appl. Mater. Interfaces* **2012**, *4*, 3285−3292.
(43) Wang, Q.; Bao, Y.; Ahire, J.; Chao, Y. *Adv. Healthcare Mater.* **2013**, *2*, 459−466.
(44) Wang, Q.; Bao, Y.; Zhang, X.; Coxon, P. R.; Jayasooriya, U. A.; Chao, Y. *Adv. Healthcare Mater.* **2012**, *1*, 189−198.
(45) Zhu, C.; Yang, Q.; Liu, L.; Lv, F.; Li, S.; Yang, G.; Wang, S. *Adv. Mater.* **2011**, *23*, 4805−4810.
(46) Sieradzki, K.; Tomasz, A. *Antimicrob. Agents Chemother.* **2006**, *50*, 527−533.